HYPERNUCLEAR CONSTRAINTS ON ΛN AND ΛNN INTERACTIONS

Eliahu Friedman, Avraham Gal

Racah Institute of Physics, The Hebrew University, Jerusalem 9190400, Israel

Received 2 September 2025, accepted 13 September 2025, published online 10 February 2026

Recent work on using density-dependent Λ-nuclear optical potentials in calculations of Λ-hypernuclear binding energies is reviewed. It is found that all known Λ binding energies in the mass range of $16 \leq A \leq 208$ are well fitted in terms of two interaction parameters: one, attractive, for the spin-averaged ΛN interaction, and another one, repulsive, for the ΛNN interaction. The ΛN interaction term by itself overbinds Λ hypernuclei, in quantitative agreement with recent findings obtained in EFT and Femtoscopy studies. The strength of the ΛNN interaction term is compatible with values required to resolve the hyperon puzzle.

DOI:10.5506/APhysPolB.57.2-A16

1. Introduction and background

Binding energies of Λ hyperons in single-particle states of Λ hypernuclei along the periodic table have been studied since the 1970s [1]. Although fitted by several Skyrme–Hartree–Fock versions, *e.g.*, Refs. [2, 3], a systematic study using microscopic density-dependent (DD) optical potentials consisting of two-body ΛN and three-body ΛNN interaction terms was lacking. The need to consider both terms in constructing a DD Λ-nucleus optical potential $V_\Lambda^{\rm opt}(\rho)$ was prompted by recent observations of neutron stars (NS) with masses exceeding twice the solar mass. Such observations appeared to be in conflict with the expectation that Λ hyperons in NS cores interacting exclusively with two-body attractive ΛN interactions would soften the NS equation of state, thereby limiting NS masses to below ~ 1.5 solar mass. This issue, named the 'hyperon puzzle', has been discussed extensively in recent years [4]. However, a mechanism of inhibiting the appearance of Λ hyperons through a repulsive ΛNN interaction apparently explains the astrophysical observations [5]. This led us to revisit the construction of a proper DD $V_\Lambda^{\rm opt}$.

The Λ binding-energy input to the present work is shown in Fig. 1 which presents a three-parameter Woods–Saxon (WS) fit to all Λ s.p. binding energies from various experiments marked in the figure. A limiting value of $B_\Lambda(A) \to 30$ MeV as $A \to \infty$ is implied by this fit, updating the original 28 MeV value from the 1988 first comprehensive data analysis [2]. However, since the chosen WS potential is not related directly to the nuclear density $\rho(r)$, the remarkable fit shown in Fig. 1 does not tell how this 30 MeV Λ-nuclear potential depth is split between ΛN two-body and ΛNN three-body contributions.

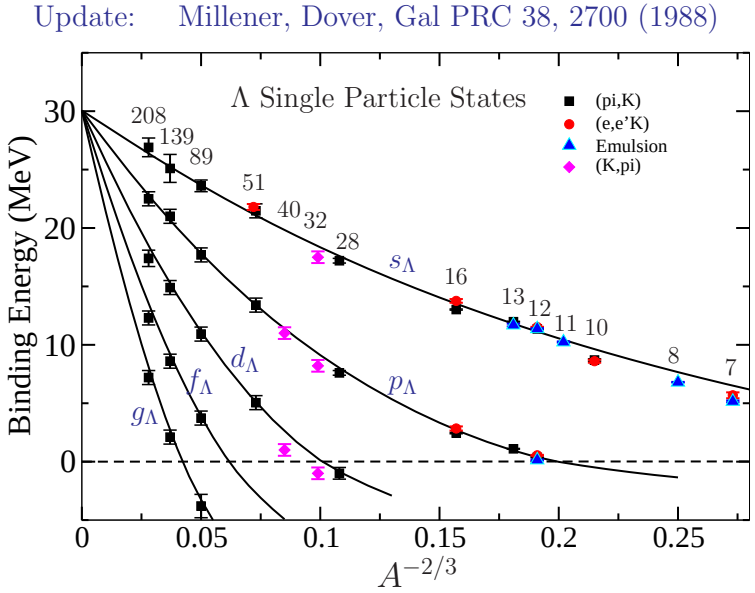

Fig. 1. A three-parameter Woods–Saxon potential fit of all known Λ single-particle binding energies from various experiments across the periodic table marked by different colors. Figure adapted from Ref. [1], updating the original figure in Ref. [2].

The present work offers a brief summary and extension of recently published work on this topic [6, 7]. In Section 2, $V_\Lambda^{\rm opt}$ is constructed in terms of nuclear densities based on nuclear sizes. Section 3 shows optical-potential predictions obtained, first by fitting its ΛN and ΛNN strength parameters to the $1s_\Lambda$ and $1p_\Lambda$ binding energies in ${}^{16}_{\Lambda}$N, and then by a χ^2 fit to $1s_\Lambda$ and $1p_\Lambda$ single-particle (s.p.) binding energies shown in Fig. 1 across the periodic table. A need to suppress the ΛNN interaction term when one of the two nucleons is an 'excess' neutron is observed, apparently related to

its isospin dependence. Section 4 demonstrates a way to substantiate the isospin dependence of the ΛNN term in ${}^{40,48}\mathrm{Ca}(e,e'K^+){}^{40,48}_{\Lambda}\mathrm{K}$ electroproduction experiments scheduled at JLab. The concluding Section 5 presents a brief discussion and summary of our optical potential methodology in comparison with other approaches. In particular, the strength of the repulsive ΛNN interaction term of $V_\Lambda^{\rm opt}$ found here is compatible with that required to resolve the hyperon puzzle [5].

2. DD optical potentials

The optical potential $V_\Lambda^{\rm opt}(\rho) = V_\Lambda^{(2)}(\rho) + V_\Lambda^{(3)}(\rho)$ consists of two-body ΛN and three-body ΛNN interaction terms

$$V_\Lambda^{(2)}(\rho) \;=\; -\frac{4\pi}{2\mu_\Lambda}\frac{f_A^{(2)}\,b_0}{1+\frac{3k_{\rm F}}{2\pi}f_A^{(2)}\,b_0}\,\rho\,, \tag{1}$$

$$V_\Lambda^{(3)}(\rho) \;=\; +\frac{4\pi}{2\mu_\Lambda}f_A^{(3)}\,B_0\,\frac{\rho^2}{\rho_0}\,, \tag{2}$$

with b_0 and B_0 strength parameters in units of fm ($\hbar = c = 1$). In these expressions, A is the mass number of the *nuclear core* of the hypernucleus, ρ is a nuclear density normalized to A, $\rho_0 = 0.17$ fm^{-3} stands for nuclear-matter density, μ_Λ is the Λ-nucleus reduced mass, and $f_A^{(2,3)}$ are kinematical factors involved in going from the ΛN and ΛNN c.m. systems, respectively, to the Λ-nucleus c.m. system

$$f_A^{(2)} = 1 + \frac{A-1}{A}\frac{\mu_\Lambda}{m_N}\,, \qquad f_A^{(3)} = 1 + \frac{A-2}{A}\frac{\mu_\Lambda}{2m_N}\,. \tag{3}$$

The novelty of this form of $V_\Lambda^{\rm opt}(\rho)$ is that its $V^{(2)}$ component accounts explicitly for Pauli correlations through its dependence on the Fermi momentum $k_F = (3\pi^2\rho/2)^{1/3}$, which strongly affects the balance between the derived values of potential parameters b_0 and B_0. In contrast, introducing Pauli correlations also in $V_\Lambda^{(3)}$ is found to make little difference, which is why it is skipped in Eq. (2). This form of including Pauli correlations was suggested in Ref. [8] and practised by us since 2013 in K^- atom [9] and η-nuclear studies [10] within a Jerusalem–Prague collaboration as reviewed in Refs. [11, 12]. We note that the ΛNN potential term $V_\Lambda^{(3)}(\rho)$ derives mostly from OPE diagrams with ΣNN and $\Sigma^* NN$ intermediate states [13], whereas NN short-range correlations are estimated to affect the derived value of B_0 by a few percent at most. Finally, the low-density limit of $V_\Lambda^{\rm opt}$ requires that b_0 is identified with the c.m. ΛN spin-averaged scattering length, taken positive here.

Regarding the nuclear densities $\rho(r) = \rho_p(r) + \rho_n(r)$ used in $V_\Lambda^{\rm opt}$, it is essential to ensure that the radial extent of the densities, *e.g.*, their r.m.s. radii, follow closely the values derived from experiment. Here, we relate the proton densities to the corresponding charge densities, where proton-charge finite size and recoil effects are included. This is equivalent to assigning some finite range to the ΛN interaction. For the lightest elements in our database, we used harmonic-oscillator type densities, assuming the same radial parameters also for the corresponding neutron densities [14]. For species beyond the nuclear $1p$ shell we used two-parameter and three-parameter Fermi distributions normalized to Z for protons and $N = A - Z$ for neutrons, derived from nuclear charge distributions assembled in Ref. [15]. For medium-weight and heavy nuclei, the r.m.s. radii of neutron density distributions assume larger values than those for protons. Furthermore, once neutrons occupy single-nucleon orbits beyond those occupied by protons, it is useful to represent the nuclear density $\rho(r)$ as

$$\rho(r) = \rho_{\rm core}(r) + \rho_{\rm excess}(r)\,, \tag{4}$$

where $\rho_{\rm core}$ refers to the Z protons plus the charge-symmetric Z neutrons occupying the same nuclear 'core' orbits, and $\rho_{\rm excess}$ refers to the $(N - Z)$ 'excess' neutrons associated with the nuclear periphery.

3. Optical-potential fits to Λ hypernuclear binding energies

Motivated by the simple $1p$ proton–hole structure of the ^{15}N nuclear core of $^{16}_{\Lambda}$N, which removes most of the uncertainty from the spin-dependent ΛN and ΛNN interactions, we started our optical-potential study of Λ hypernuclei by fitting $B_\Lambda(1s)$ and $B_\Lambda(1p)$ in $^{16}_{\Lambda}$N. The fit parameters are $b_0 = 1.53$ fm, $B_0 = 0.22$ fm, and the corresponding partial potential depths and total depth at nuclear-matter density $\rho_0 = 0.17$ fm^{-3} for $A \to \infty$ are

$$D_\Lambda^{(2)} = -39.3 \text{ MeV}\,, \qquad D_\Lambda^{(3)} = +13.1 \text{ MeV}\,, \qquad D_\Lambda = -26.2 \text{ MeV}\,. \tag{5}$$

Next, we show in the top part of Fig. 2 (model X) results of using the Λ optical-potential strength parameters b_0 and B_0 of Eqs. (1) and (2), determined by fitting to $^{16}_{\Lambda}$N $1s_\Lambda$ and $1p_\Lambda$ binding energies, in calculations of *all* $1s_\Lambda$ and $1p_\Lambda$ pairs of binding energies along the periodic table. Clearly seen is the underbinding of $1s_\Lambda$ and $1p_\Lambda$ states in the heavier hypernuclei, which could result from treating equally all NN pairs, including pairs where one nucleon is in the nuclear 'core', while the other is an 'excess' neutron. Removing this bilinear term from ρ^2, using Eq. (4), we replace ρ^2 beyond ^{40}Ca with

$$\rho^2_{\rm core} + \rho^2_{\rm excess} \to (2\rho_p)^2 + (\rho_n - \rho_p)^2\,, \tag{6}$$

approximated in terms of the available densities ρ_p and ρ_n. This prescription is suggested by the $\vec{\tau}_1 \cdot \vec{\tau}_2$ isospin dependence that arises from intermediate Σ and Σ^* hyperons in the ΛNN OPE interaction [13]. The associated effect of weakening the repulsive ΛNN term beyond ^{40}Ca is seen in the lower part of Fig. 2 (model Y).

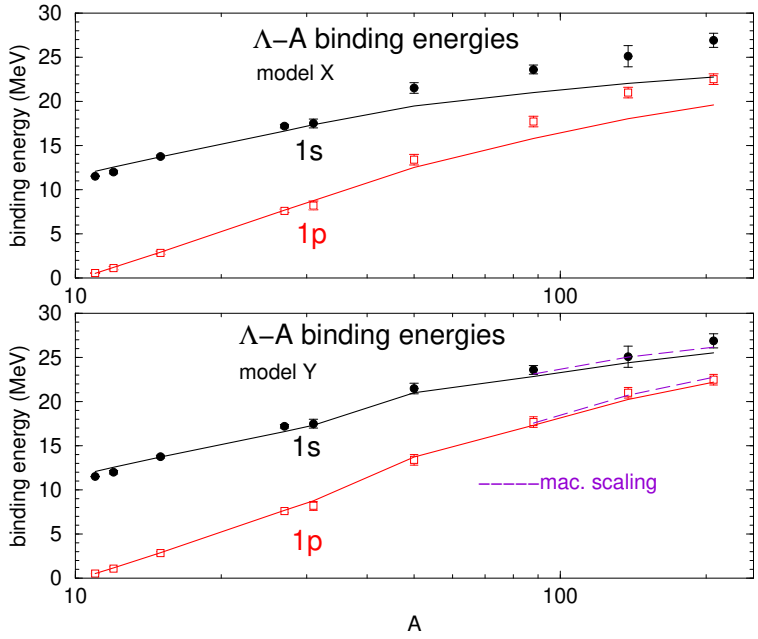

Fig. 2. $B_\Lambda^{1s,1p}(A)$ values across the periodic table, $12 \leq A \leq 208$ as calculated in models X (upper) and Y (lower), compared with data points, including uncertainties. $^{16}_{\Lambda}$N is the third point on each line. Continuous lines connect calculated values. Figure updating Fig. 3 in Ref. [6]. The upper part, model X, uses the full ρ^2 term. The lower part, model Y, replaces ρ^2 with a reduced form, decoupling $(N-Z)$ excess neutrons from $2Z$ symmetric-core nucleons, see the text. The dashed lines are for ρ^2 replaced with $F\rho^2$, with a suppression factor F, Eq. (7).

In order to simplify things, one may multiply ρ^2 by a suppression factor

$$F = \frac{(2Z)^2 + (N-Z)^2}{A^2}\,. \tag{7}$$

This suppression factor, approximately the ratio of the volume integral of $(2\rho_p)^2 + (\rho_n - \rho_p)^2$ to that of ρ^2, becomes significant for heavy hypernuclei, with as small value as $F = 0.67$ for Pb. Results using $F\rho^2$ instead of Eq. (6) are shown in the lower part of the figure as dashed lines ('mac. scaling'), leading to almost identical values for these two options.

At the next stage, we performed full χ^2 fits with the suppression factor F included for the four heaviest species. Figure 3 shows several fits to the ($1s_\Lambda$, $1p_\Lambda$) B_Λ data, where black solid lines show fits to the full data set and open circles with error bars mark B_Λ data points listed in Table IV of Ref. [1], including experimental uncertainties, and summarized in Table 2 of Ref. [7]. It is clearly seen that the $1s_\Lambda$ states in ${}^{12}_{\Lambda}$B and ${}^{13}_{\Lambda}$C do not fit into the otherwise good agreement with experiment for the heavier species. The red dashed lines show a very good fit obtained upon excluding these two light elements from the B_Λ data set. In fact, the potential parameters b_0 and B_0 of Eqs. (1), (2) are hardly affected by the ${}^{12}_{\Lambda}$B and ${}^{13}_{\Lambda}$C B_Λ input. The fit parameters are $b_0 = 1.446 \pm 0.088$ fm, $B_0 = 0.193 \pm 0.022$ fm, with 100% correlation between the two parameters. The corresponding fully correlated partial potential depths, and the full one, at nuclear-matter density $\rho_0 = 0.17$ fm^{-3} are (in MeV)

$$D_\Lambda^{(2)} = -38.6 \mp 0.8\,, \qquad D_\Lambda^{(3)} = 11.5 \pm 1.4\,, \qquad D_\Lambda = -27.1 \pm 0.6\,. \quad (8)$$

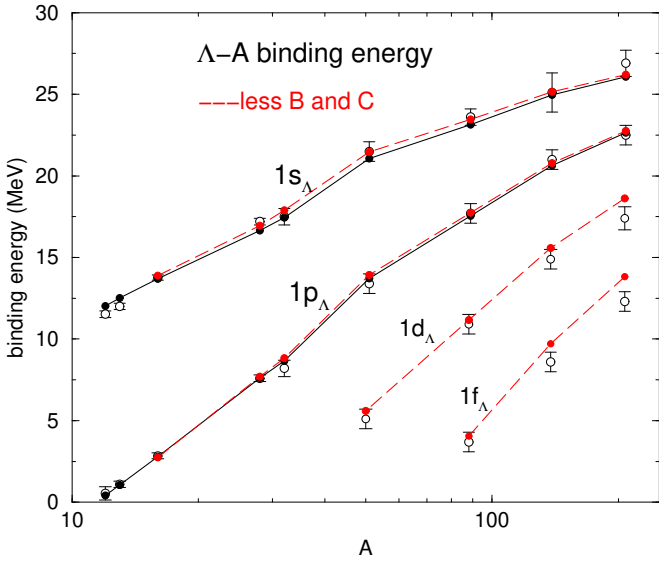

Fig. 3. χ^2 fits to the full $1s_\Lambda$ and $1p_\Lambda$ data (solid black lines) and when excluding ${}^{12}_{\Lambda}$B and ${}^{13}_{\Lambda}$C (dashed red lines). Also shown are *predictions* of $1d_\Lambda$ and $1f_\Lambda$ binding energies for the latter choice.

Also included in Fig. 3 are *predictions* of $1d_\Lambda$ and $1f_\Lambda$ binding energies made with these parameters. Although it is not expected that such states will be well described by the same potential, owing to overlooked secondary effects such as non-local terms, it is seen that while slight overbinding of the calculated energies appears for the heavier species, the present optical potential reproduces quite well the four lowest Λ single-particle states in neutron-rich hypernuclei. It is therefore of interest to repeat the χ^2 process on the whole set of experimental binding energies of Λ single-particle states, a total of 21 binding-energy values between ${}^{16}_{\Lambda}$N and ${}^{208}_{\Lambda}$Pb. The resulting χ^2 per degree of freedom is then 0.95 (compared to 0.6 from a fit to only 14 binding-energy values for the $1s_\Lambda$ and $1p_\Lambda$ states) and the potential parameters are $b_0 = 1.32 \pm 0.071$ fm, $B_0 = 0.164 \pm 0.020$ fm, and are 100% correlated. The corresponding fully correlated partial potential depths and the full one at nuclear-matter density $\rho_0 = 0.17$ fm^{-3} are (in MeV)

$$D_\Lambda^{(2)} = -37.4 \mp 0.7\,, \qquad D_\Lambda^{(3)} = 9.8 \pm 1.2\,, \qquad D_\Lambda = -27.6 \pm 0.5\,. \tag{9}$$

These values are in agreement with those in Eq. (8) based only on $1s_\Lambda$ and $1p_\Lambda$ states. The uncertainties in the parameter values quoted above are statistical only. To estimate systematic effects within the adopted model, we repeated the analysis with slightly modified nuclear densities such as those obtained when unfolding the finite size of the proton. Values of b_0 came out unchanged, whereas values of B_0 increased typically by 0.015 fm. The total potential depth at $\rho_0 = 0.17$ fm^{-3} changed to $D_\Lambda = -26.8 \pm 0.4$ MeV, suggesting a systematic uncertainty of somewhat less than 1 MeV for this value.

4. Test of isospin dependence

Having imposed on our B_Λ optical-potential fits the isospin-related suppression factor F, Eq. (7), we discuss here a test case which demonstrates its effect on Λ hypernuclear spectra. Figure 4 shows calculated differences of B_Λ values for the $1s_\Lambda$ and $1p_\Lambda$ states between ${}^{48}_{\Lambda}$K and ${}^{40}_{\Lambda}$K as a function of the neutron skin $r_n - r_p$ in ${}^{48}_{\Lambda}$K. The upper/lower part of the figure shows predictions made using $V_\Lambda^{\rm opt}$ upon including/excluding the suppression factor F. Regardless of the chosen value of $r_n - r_p$, the effect of applying F is about 2.5 MeV for the $1s_\Lambda$ state and more than 2 MeV for the $1p_\Lambda$ state, both are within reach of the $(e, e'K^+)$ approved JLab E12-15-008 experiment on ^{40,48}Ca targets [16]. For $F = 1$, our calculated B_Λ values are close to those calculated in Refs. [17–19].

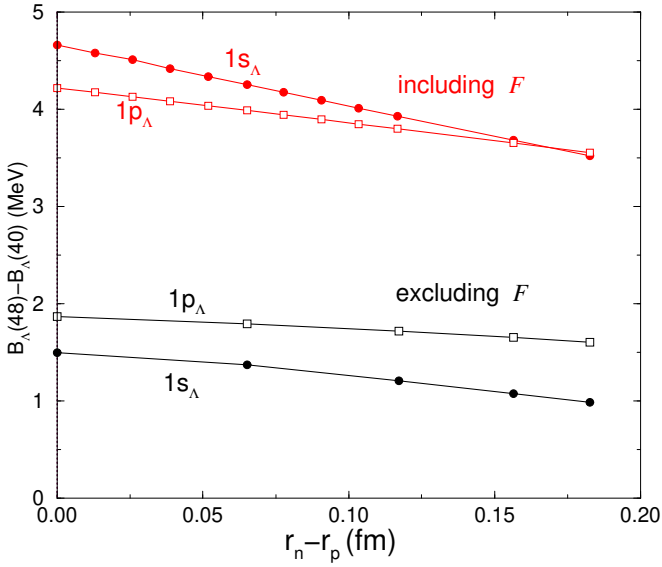

Fig. 4. $B_\Lambda(^{48}_{\Lambda}\mathrm{K}) - B_\Lambda(^{40}_{\Lambda}\mathrm{K})$ values for $1s_\Lambda$ and $1p_\Lambda$ states, with and without applying the suppression factor F, as a function of the neutron-skin of $^{48}_{\Lambda}$K, see the text.

5. Discussion and summary

First, we discuss briefly the effect of Pauli correlations entered in $V_\Lambda^{(2)}(\rho)$, Eq. (1), by the renormalization factor $\mathrm{PC} = (1 + \frac{3k_\mathrm{F}}{2\pi} f_A^{(2)}\, b_0)^{-1}$. In Table 1, we list values of partial potential depths $D_\Lambda^{(2)}$ and $D_\Lambda^{(3)}$ determined by fitting $B_\Lambda(1s)$ and $B_\Lambda(1p)$ in $^{16}_{\Lambda}$N with/without PC. The total depth, as expected, is practically the same in both derivations. The difference in the partial potential depths is traced to the treatment of Pauli correlations. Expanding PC in powers of $k_F \propto \rho^{1/3}$, its repulsive ρ term along with the overall ρ factor in $V_\Lambda^{(2)}$ produce a repulsive ρ^2 term in $V_\Lambda^{(2)}(\rho)$, thereby enhancing $V_\Lambda^{(3)}(\rho) \propto \rho^2$ which then boosts $D_\Lambda^{(3)}$. Finally, to keep the total depth D_Λ

Table 1. Comparison of two-body, three-body, and total Λ-nucleus potential depths at nuclear matter density $\rho_0 = 0.17$ fm^{-3} obtained by fitting b_0 and B_0 to $B_\Lambda(1s)$ and $B_\Lambda(1p)$ in $^{16}_{\Lambda}$N with and without considering Pauli correlations; see the text.

Model	$D_\Lambda^{(2)}$ [MeV]	$D_\Lambda^{(3)}$ [MeV]	D_Λ [MeV]
with PC [6]	−39.3	+13.1	−26.2
w/o PC [2]	−57.8	+31.4	−26.4

about the same, $|D_\Lambda^{(2)}|$ must increase too. A similar effect of boosting both values of $|D_\Lambda^{(2)}|$ and $D_\Lambda^{(3)}$ is seen also in Skyrme–Hartree–Fock (SHF) analyses of Λ s.p. binding energies, *e.g.*, Refs. [2, 3], which treat Pauli correlations incompletely.

Results of various Λ-nuclear potential-depth calculations are listed in Table 2, divided into two groups. The first group consists of recent calculations, mostly EFT, confirming that ΛN interactions overbind Λ hypernuclei by as much as about 10 MeV, a value consistent with a ΛNN repulsive contribution of order 10 MeV in order to satisfy the total potential depth value $D_\Lambda \approx -27$ MeV suggested by the overall B_Λ data. The second group demonstrates our own $V_\Lambda^{\rm opt}$ determination of Λ-nuclear partial potential depths, Eqs. (8) and (9). Our fitted value of the ΛNN potential depth, $D_\Lambda^{(3)} \approx 10$ MeV, agrees with the ΛNN potential strength derived in the Gerstung–Kaiser–Weise calculation [5] which appears to resolve the hyperon puzzle.

Table 2. Two-body, three-body, and total Λ-nucleus potential depths (in MeV) at nuclear matter density $\rho_0 = 0.17$ fm^{-3} from several model calculations and from hypernuclear binding-energy data ($\mathcal{N}$ stands for the number of data points).

Model	$D_\Lambda^{(2)}$	$D_\Lambda^{(3)}$	D_Λ
Nijmegen ESC16,16$^+$ [20]	-43.7	$+5.8$	-37.9
EFT NLO19 [21]	-39 to -29	—	—
NLO19 + **10** dominance [5]	≈ -36	$\approx +10$	
EFT N^{2}LO [22]	-33 to -38	—	—
Femtoscopy [23]	$-36.3 \pm 1.3^{+2.5}_{-6.2}$	—	—
$V_\Lambda^{\rm opt}$ [present] ($\mathcal{N} = 14$)	-38.6 ∓ 0.8	11.5 ± 1.4	-27.1 ± 0.6
$V_\Lambda^{\rm opt}$ [present] ($\mathcal{N} = 21$)	-37.4 ∓ 0.7	9.8 ± 1.2	-27.6 ± 0.5

REFERENCES

[1] A. Gal, E.V. Hungerford, D.J. Millener, «Strangeness in nuclear physics», *Rev. Mod. Phys.* **88**, 035004 (2016).

[2] D.J. Millener, C.B. Dover, A. Gal, «Λ-nucleus single-particle potentials», *Phys. Rev. C* **38**, 2700 (1988).

[3] H.-J. Schulze, E. Hiyama, «Skyrme force for light and heavy hypernuclei», *Phys. Rev. C* **90**, 047301 (2014).

[4] L. Tolos, L. Fabbietti, «Strangeness in nuclei and neutron stars», *Prog. Part. Nucl. Phys.* **112**, 103770 (2020).

[5] D. Gerstung, N. Kaiser, W. Weise, «Hyperon–nucleon three-body forces and strangeness in neutron stars», *Eur. Phys. J. A* **56**, 175 (2020).

[6] E. Friedman, A. Gal, «Constraints from Λ hypernuclei on the ΛNN content of the Λ nucleus potential», *Phys. Lett. B* **837**, 137669 (2023).

[7] E. Friedman, A. Gal, «Λ hypernuclear potentials beyond linear density dependence», *Nucl. Phys. A* **1039**, 122725 (2023).

[8] T. Waas, M. Rho, W. Weise, «Effective kaon mass in dense baryonic matter: role of correlations», *Nucl. Phys. A* **617**, 449 (1997).

[9] E. Friedman, A. Gal, «Kaonic atoms and in-medium K^-N amplitudes II: Interplay between theory and phenomenology», *Nucl. Phys. A* **899**, 60 (2013).

[10] E. Friedman, A. Gal, J. Mareš, «η-nuclear bound states revisited», *Phys. Lett. B* **725**, 334 (2013).

[11] E. Friedman *et al.*, «Studies of mesic atoms and nuclei», *PoS* **(Hadron2017)**, 195 (2018).

[12] N. Barnea *et al.*, «Onset of η nuclear binding», *EPJ Web Conf.* **181**, 01011 (2018).

[13] A. Gal, J.M. Soper, R.H. Dalitz, «Shell-model analysis of Λ binding energies for p-shell hypernuclei. I. Basic formulas and matrix elements for ΛN and ΛNN forces», *Ann. Phys. (NY)* **63**, 53 (1971).

[14] L.R.B. Elton, «Nuclear Sizes», *Oxford University Press*, Oxford 1961.

[15] I. Angeli, K.P. Marinova, «Table of experimental nuclear ground state charge radii: An update», *At. Data Nucl. Data Tables* **99**, 69 (2013).

[16] S.N. Nakamura, «Future prospects of spectroscopic study of Λ hypernuclei at JLab and J-PARC HIHR», *EPJ Web Conf.* **271**, 11003 (2022).

[17] M. Isaka, Y. Yamamoto, Th.A. Rijken, «Effects of a hyperonic many-body force on B_Λ values of hypernuclei», *Phys. Rev. C* **95**, 044308 (2017).

[18] P. Bydžovsky *et al.*, «Self-consistent many-body approach to the electroproduction of hypernuclei», *Phys. Rev. C* **108**, 024615 (2023).

[19] P. Bydžovsky, D. Denisova, F. Knapp, P. Veselý, «Electroproduction of medium- and heavy-mass hypernuclei», *Phys. Rev. C* **112**, 024609 (2025).

[20] M.M. Nagels, Th.A. Rijken, Y. Yamamoto, «Extended-soft-core baryon–baryon model ESC16. II. Hyperon–nucleon interactions», *Phys. Rev. C* **99**, 044003 (2019).

[21] J. Haidenbauer, U.-G. Meißner, A. Nogga, «Hyperon–nucleon interaction within χEFT revisited», *Eur. Phys. J. A* **56**, 91 (2020).

[22] J. Haidenbauer, U.-G. Meißner, A. Nogga, H. Le, «Hyperon–nucleon interaction in χEFT at N^{2}LO», *Eur. Phys. J. A* **59**, 63 (2023).

[23] D.L. Mihaylov, J. Haidenbauer, V. Mantovani Sarti, «Constraining the $p\Lambda$ interaction from a combined analysis of scattering data and correlation functions», *Phys. Lett. B* **850**, 138550 (2024).